Inorganica Chimica Acta 383 (2012) 169–177

Contents lists available at SciVerse ScienceDirect

Inorganica Chimica Acta

journal homepage: www.elsevier.com/locate/ica

Novel boron compounds of 2,3- and 2,5-pyridinedicarboxylic acids

Alper Tolga Çolak [a,*], Yüksel Şahin [b], Okan Zafer Yeşilel [c], Ferdağ Çolak [d], Filiz Yılmaz [e], Murat Taş [f]

[a] Department of Chemistry, Faculty of Arts and Sciences, Dumlupınar University, 43820 Kütahya, Turkey
[b] Department of Chemistry, Faculty of Arts and Sciences, Adnan Menderes University, 09010 Aydın, Turkey
[c] Department of Chemistry, Faculty of Arts and Sciences, Eskişehir Osmangazi University, 26480 Eskişehir, Turkey
[d] Department of Biology, Faculty of Arts and Sciences, Dumlupınar University, 43820 Kütahya, Turkey
[e] Department of Chemistry, Science Faculty, Anadolu University, 26470 Eskişehir, Turkey
[f] Department of Chemistry, Faculty of Arts and Sciences, Giresun University, 28049 Giresun, Turkey

ARTICLE INFO

Article history:
Received 16 February 2011
Received in revised form 28 October 2011
Accepted 2 November 2011
Available online 15 November 2011

Keywords:
2,3-Pyridinedicarboxylate
2,5-Pyridinedicarboxylate
Boron compound
Diphenylborinic acid
Antimicrobial activity
MIC

ABSTRACT

The (Hea)[B(ph)$_2$(2,3-pydc)] (**1**) and (Hea)[B(ph)$_2$(2,5-pydc)] (**2**) boron compounds (2,3-H_2pydc = 2,3-pyridinedicarboxylic acid, 2,5-H_2pydc = 2,5-pyridinedicarboxylic acid, Hea = ethanolammonium) were synthesized and characterized by elemental analysis, spectroscopic measurements (UV–Vis, ^{11}B NMR, ^{13}C NMR, ^{1}H NMR and IR spectra) and single crystal X-ray diffraction technique. Compound **1** and **2** crystallize in the monoclinic space group P2$_1$/c. The crystal packing of compound **1** is stabilized through strong intermolecular hydrogen bonding and C–H···π interactions, resulting in a 3D framework. The individual molecules of **2** are connected by the N–H···O and O–H···O hydrogen bonds leading to two-dimensional hydrogen bonded layer. The *in vitro* antibacterial and anticandidal activities of (**1**) and (**2**) were evaluated by disc diffusion method and MIC tests. Both new complexes showed antimicrobial activity against MRSA and clinical and standard yeast isolates.

1. Introduction

The chemistry of elemental boron, its compounds and crystalline phases based on them is currently a vast and quite complicated scientific field at the boundary of inorganic and organo-element chemistry. Boron compounds are successfully used in various areas of materials science, in catalysis, surface chemistry, inorganic and organic synthesis, biochemistry, agriculture, medicine, forestry and OLEDs [1–7]. The synthesis of boron derivatives of biomolecules such as amino acids, peptides, nucleosides, porphyrins and sugars is a major area of research [8]. For the past decade chemists have been interested in the synthesis and characterization of five- and six-membered boron compounds with a coordinative N → B bond. Also such boron compounds have been prepared from pyridinedicarboxylic acids [9–13]. These acids can act as both a multiple proton donor and an acceptor while also using their carboxylate oxygen and nitrogen atoms, which are highly accessible to metal ions, to form interesting network structures [14,15]. Pyridinedicarboxylic acids have widely been used as organic ligands for the construction of organic–inorganic hybrid materials, which have been of great interest in recent years [16–22]. These types of ligands combine the advantages of both organic multi-carboxylic acid and aromatic compounds. 2,3- and 2,5-pyridinedicarboxylic acids with divergent function groups, which possibly form bridging hydrogen bonds, are interesting and have potential for self-assembly. In addition, the carboxylic groups in position 5 of the pyridine ring may be prone to involvement in hydrogen bonds [23,24]. Organic boron compounds can be studied by multinuclear NMR techniques. Particularly, ^{11}B NMR provides valuable structural information due to its sensitivity to electronic and steric effects as well as to the boron coordination number. The structures of several new compounds have been determined by X-ray diffraction analyses [25].

Herein, we report the synthesis, characterization and antimicrobial activity of two novel boron compounds, using 2,3- and 2,5-pyridinedicarboxylic acids involving coordinative N → B bonds.

2. Experimental

2.1. Materials and measurements

All chemicals and solvents used for the syntheses were of reagent grade. The synthesis of diphenylborinic acid was carried out under an atmosphere of dry argon by using standard Schlenk techniques. ^{1}H and ^{13}C NMR spectra were recorded with Varian AS 400. ^{11}B NMR spectra were recorded with a Varian AS 600 spectrometer. NMR references were $(CH_3)_4Si$ and $BF_3{\cdot}Et_2O$. 2,3-Pyridinedicarboxylic acid and 2,5-pyridinedicarboxylic acid (Aldrich) were used as received. Elemental analysis (C, H, and N) was performed using a Vario EL III CHNS elemental analyzer.

* Corresponding author. Tel.: +90 2742652051; fax: +90 2742652056.
E-mail address: acolak@dumlupinar.edu.tr (A.T. Çolak).

0020-1693/$ - see front matter © 2011 Elsevier B.V. All rights reserved.
doi:10.1016/j.ica.2011.11.006

FT-IR spectra were recorded in the 4000–400 cm^{-1} region with a Bruker Optics, Vertex 70 FT-IR spectrometer using KBr pellets. Thermal analyses were performed by the Seiko S II TG-DTA-DTG system, in a dynamic nitrogen atmosphere (200 mL/min), at a heating rate of 3 °C/min, in the temperature range of 35–1300 °C in platinum sample vessels with reference to α-Al_2O_3.

2.2. Crystallographic analyses

Diffraction data for complexes were collected with a Bruker AXS APEX [26] CCD diffractometer equipped with a rotation anode at 100(2) K using graphite monochrometed Mo Kα radiation (l = 0.71069 Å). Diffraction data were collected over the full sphere and were corrected for absorption. The data reduction was performed with the SAINT program package. For further crystal and data collection details see Table 2. Structure solution was found with the SHELXS-97 [27] package using the direct-methods and was refined SHELXL-97 [28] against F2 using first isotropic. All non-hydrogen atoms were refined anisotropically. Hydrogen atoms were added to the structure model at calculated positions. Geometric calculations were performed with Platon [29]. Molecular drawings were obtained using Mercury [30]. The H atom of O–H in 2-ammoniumethanol was found from a difference Fourier map and was refined with distance restraint of O–H = 0.8 Å. The remaining H atoms including N–H atoms in 2-ammoniumethanol were refined using a riding model with Uiso(H) = 1.2 Ueq(C).

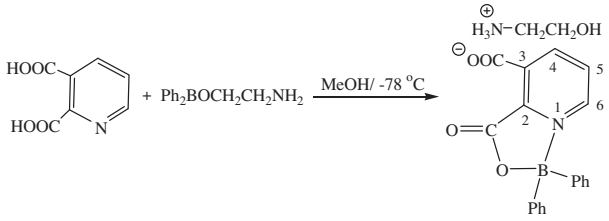

Scheme 1. Synthesis of **1**.

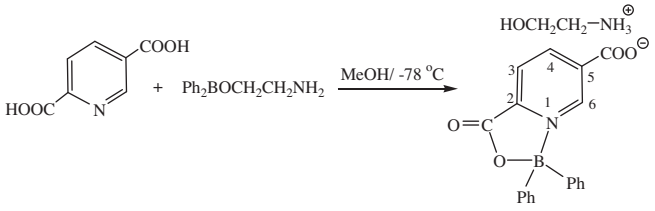

Scheme 2. Synthesis of **2**.

2.3. Biological evaluation

2.3.1. Antimicrobial assays

2.3.1.1. Microorganisms and media. The antimicrobial activities were tested against clinical microorganisms of Gram positive (methicillin-resistant *Staphylococcus aureus*) and Gram negative (Vancomycin resistant *Enterococcus faecium*) bacteria and yeasts (*Candida albicans* (3 isolates), *Candida krusei*, *Candida glabrata*, *Candida parapsilosis* and *Candida tropicalis*). The clinical isolates were obtained from hospitalised patients, and were a kind gift from the Microbiology Laboratory of the Faculty of Medicine, University of Eskişehir, Osmangazi, Turkey and the State Hospital of Kütahya, Turkey. The standard strains used in the experiment were *S. aureus* ATCC 25923, *Bacillus subtilis* NRRL 209, *Bacillus cereus* NRRL 3711, *Escherichia coli* ATCC 25922, *Aeromonas hydrophilia* NRRL 406, *Proteus vulgaris* NRRL-B 123, *Enterococcus fecalis* ATCC 29212, *Saccharomyces baulardii*, *Rhodotorula rubra* DSM 70403 and *C. albicans* NRRL Y-12983. The standard strains were obtained from the American Type Culture Collection (Rock-ville, MD, USA) and Northern Regional Research Laboratory (USDA, Peoria, IL, USA). Cultures of each microbial species were maintained on Nutrient Agar medium and stored at 4 °C.

2.3.1.2. Preparation of inoculum. Cultures less than 30 h old were touched with a loop and transferred to sterile nutrient Broth. The broth was incubated at 37 °C until the growth reached a turbidity equal to or greater than that of 0.5 Mc Farland standard (at 625 nm, 0.08–0.1 absorbance). The density of microorganism suspensions was adjusted to 0.5 Mc Farland with sterile saline. The cell suspensions containing 10^8 CFU/mL cells for bacteria, 10^7 CFU/mL cells for yeasts were prepared. Inocula of the microorganisms were adjusted to a concentration of 10^5 CFU/mL for MIC assay.

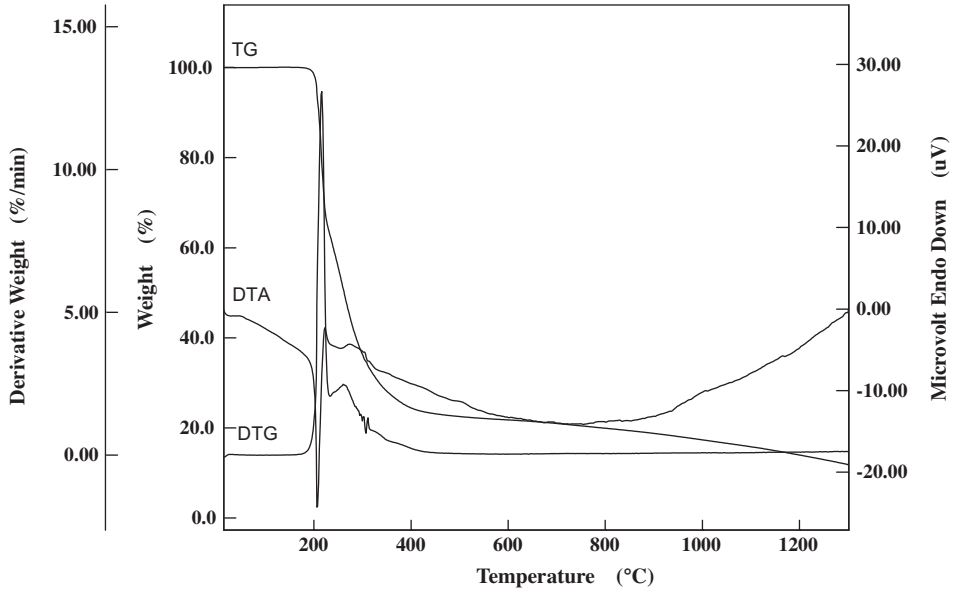

Fig. 1. TG-DTA-DTG curves of **1**.

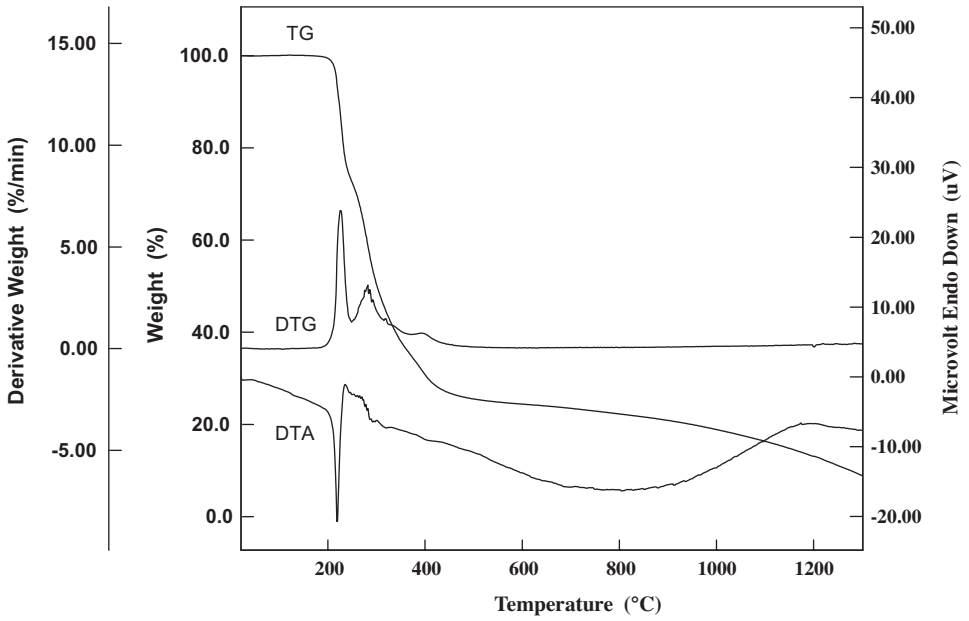

Fig. 2. TG-DTA-DTG curves of **2**.

Table 1
Crystal data and structure refinement parameters for **1** and **2**.

	1	**2**
Empirical formula	$C_{21}H_{21}BN_2O_5$	$C_{21}H_{21}BN_2O_5$
Formula weight	392.21	392.21
Temperature (K)	293 (2)	
Wavelength (Å)	0.71073 Mo Kα	
Crystal system	monoclinic	monoclinic
Space group	$P2_1/c$	$P2_1/c$
a (Å)	17.258	12.363
b (Å)	9.258	17.452
c (Å)	12.821	13.406
β (°)	108.03	138.19
V (Å^3)	1948	1928
Z	4	4
D_{calc} (Mg m^{-3})	1.337	1.351
Total reflections	18030	17952
Independent reflections	4817	4825
Absorption correction	Integration	
Refinement method	Full-matrix least-squares on F^2	
R_{int}	0.035	0.063
$R[F^2 > 2\sigma(F^2)]$	0.041	0.059
$wR(F^2)$	0.104	0.207
Goodness-of-fit on F^2	1.05	1.09
$\Delta\rho$ (eÅ^{-3})	0.36; −0.24	0.46; −0.51
Data/restraints/parameters	4817/0/266	4825/3/291

Table 2
Selected geometric parameters (Å, °) for **1** and **2**.

	1	**2**
Bond length		
B1–O1	1.527 (2)	1.525 (4)
B1–N1	1.595 (2)	1.624 (4)
B1–C1	1.600 (2)	1.603 (4)
B1–C7	1.613 (2)	1.609 (4)
Bond angles		
O1–B1–N1	97.7 (1)	97.3 (2)
O1–B1–C1	110.7 (1)	110.1 (2)
N1–B1–C1	113.8 (1)	111.0 (2)
O1–B1–C7	110.3 (1)	108.7 (2)
N1–B1–C7	108.6 (1)	109.7 (2)
C1–B1–C7	114.6 (1)	118.0 (2)

2.3.1.3. Assays. Agar disc diffusion method was employed for determination of the antimicrobial activity of the synthesized complexes [31]. Fresh stock solutions of the complexes were prepared in dimethylsulfoxide (DMSO) according to the three concentrations (100, 150 and 200 μg/disc) for activity experiments. DMSO was used as negative control. Fifteen millilitres of the nutrient agar (45 °C) was poured into sterile Petri dishes (Ø 90 mm). The plates were dried for 2 days at room temperature. The cell suspensions containing 10^8 CFU/mL cells for bacteria, 10^7 CFU/mL cells for yeasts were prepared and were evenly spread onto the surface of the agar plates using swab sticks. The paper disc (Ø 6 mm) impregnated with 10 μL of the complexes was placed on the surface of the inoculated agar plate. The plates were preincubated for 2 h at room temperature prior to incubation at 37 °C for 24 h for bacterial

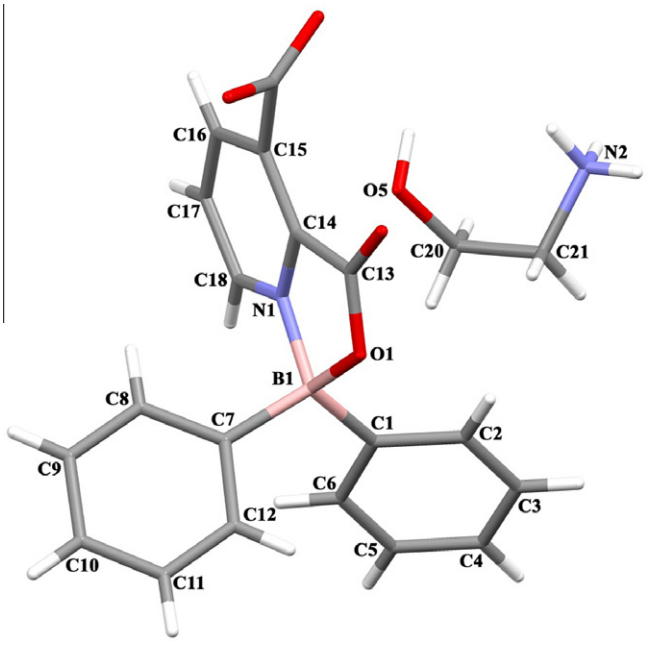

Fig. 3. The molecular structure of **1** with atom-labelling scheme.

strains and 48 h for yeast. Vancomycin (VA; 30 μg/disc), Erythromycin (E; 15 μg/disc), Chloramphenicol (C; 30 μg/disc), Imipenem (IPM; 10 μg/disc), Rifampicin (RD; 5 μg/disc, Kanamycin (K; 30 μg/disc), Cefotaxime (CTX; 30 μg/disc), Ampicillin (AMP; 10 μg/disc), Tetracycline (T; 15 μg/disc), Streptomycin (S; 25 μg/disc) and Gentamicin (CN; 30 μg/disc) for bacteria and Nystatin (N; 100 U/disc) for yeast were used as positive controls. Each assay in this experiment was repeated three times. Antimicrobial activity was evaluated by measuring the zone (mm) of inhibition against the test organisms.

Table 3
Selected hydrogen-bond geometric parameters (Å, °) for **1** and **2**.

D–H···*A*	*D*–H	H···*A*	*D*···*A*	∠*D*–H···*A*
Compound ***1***				
N2–H22A···O3^{i}	0.89	1.97	2.763 (1)	147
N2–H22B···O2^{i}	0.89	2.18	2.953 (1)	145
O5–H10···O3^{ii}	0.92 (2)	1.80 (2)	2.715 (2)	173 (1)
N2–H22C···O4^{iii}	0.89	1.90	2.790 (1)	175
Compound ***2***				
N2–H2C···O2^{i}	0.96 (4)	2.10 (4)	2.953 (4)	148 (3)
N2–H2A···O4^{ii}	0.88 (1)	1.91 (2)	2.755 (4)	163 (3)
O5–H5···O3^{iii}	0.80 (4)	1.94 (4)	2.722 (3)	167 (4)

Symmetry codes: (i) $-x+1, y-1/2, -z+1/2$; (ii) $-x+2, -y, -z+1$; (iii) $-x+1, -y, -z$.

2.4. Minimal inhibitory concentration (MIC)

In determination of the minimal inhibitory concentration of the complexes, tube dilution method was employed [32,33]. Sterile tubes were filled with 1 mL of serial two fold dilutions (500–15.6 μg/mL) of the two complexes. The nutrient broth (1 mL), containing the microorganisms was transferred into each test tube. Tubes were incubated at 37 °C for 48 h. Afterwards MIC was defined as the lowest concentration of the complexes at which the microorganisms did not demonstrate visible growth. The growth of microorganisms was indicated by the presence turbidity and a "pellet" on the tube bottom.

2.5. Minimal microcidal concentration (MMC)

The Minimal microcidal concentration (MMC) is defined as the concentration producing a ⩾99.9% reduction in CFU number in the initial inoculum. For the determination of MMC, a portion of the liquid (10 μL) from each tube that showed no turbidity was placed

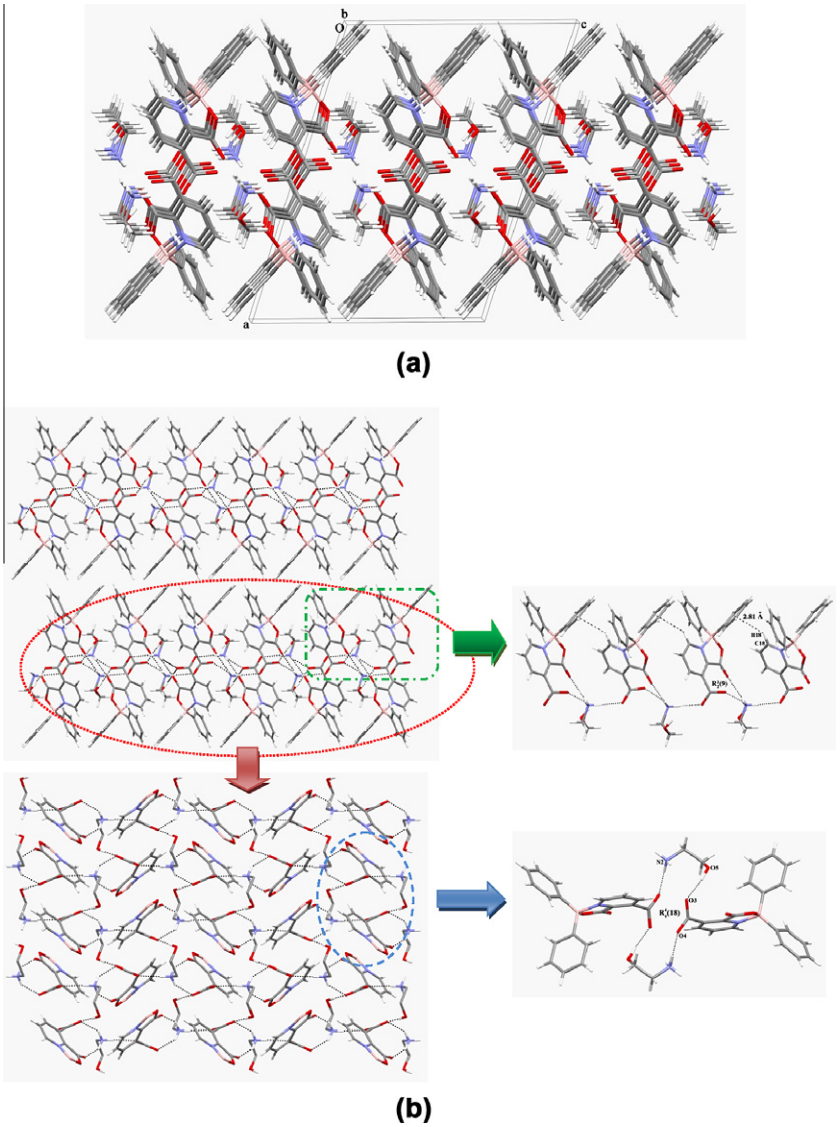

Fig. 4. (a) Unit cell and (b) The crystal packing and inter-molecular hydrogen bonding, C–H···π interactions of compound **1**.

on NA. Prior to the drying of the spots, plates were inverted and incubated at 37 °C for 62 h. The lowest concentration that yielded no growth after this sub-culturing was taken as the MMC. Both MIC and MMC were confirmed by the two replicates.

2.6. Preparation of boron compounds

2.6.1. Synthesis of diphenyl [(2-(3-carboxypyridyl))-carbonyloxy-O, N] boron (*1*) and diphenyl [(2-(5-carboxypyridyl))-carbonyloxy-O, N] boron (*2*)

1 was synthesized from a mixture of 0.60 g (3.60 mmol) of 2,3-pyridinedicarboxylic acid, and methyl diphenylborinate prepared from 0.90 g (4.00 mmol) of 2-aminoethyl diphenylborinate in 40 mL methanol at −78 °C. After evaporation of the solvent the colorless crude products were washed with a mixture of pentane–hexane (1:1) and crystallized from ethanol at 4 °C. **2** was synthesized using the same method as described for **1** using 2,5-pyridinedicarboxylic acid instead of 2,3-pyridinedicarboxylic acid in methanol at −78 °C.

2.6.1.1. Analytical data. Compound **1** (392.21 g/mol), *Anal.* Calc. for $C_{21}H_{21}BN_2O_5$: C, 64.25; H, 5.35; N, 7.14. Found: C, 64.27; H, 5.28; N, 7.17%. Yield 82%, M.p. 215–217 °C. ^{1}H (400 MHz. DMSO-d_8) δ (ppm): 2.82 (t, 2H, CH_2NH_3), 3.55 (t, 2H CH_2OH), 7.18–7.23 (m, 10 H, o-, m- and p-$2C_6H_5$), 7.98 (t, 1H, H-5), 8.15 (br, 3H, NH_3), 8.23 and 8.87 (each d, each 1H, H-4 and H-6, ^2J(H–H) = 8.0 Hz); ^{13}C (100.47 MHz, DMSO-d_8) δ (ppm): 41.3 (CH_2NH_3), 57.6 (CH_2OH), 127.0 (p-C_6H_5), 127.5 (m-C_6H_5), 130.3 (C-5), 131.8 (o-C_6H_5), 135.6 (C-3), 140.6 (C-2), 140.9 (C-6), 141.2 (C-4), 145.3 (br, i-C, C_6H_5), 162.5 (COOH), 166.8 (CO); ^{11}B (86.6 MHz, DMSO-d_6) δ (ppm): 10.2.

2.6.1.2. Analytical data. Compound **2** (392.21 g/mol), *Anal.* Calc. for $C_{21}H_{21}BN_2O_5$: C, 64.25; H, 5.35; N, 7.14. Found: C, 64.29; H, 5.31; N, 7.10%. Yield 80%, M.p. 217–219 °C. ^{1}H (400 MHz. DMSO-d_8) δ (ppm): 2.84 (t, 2H, CH_2NH_3), 3.54 (t, CH_2OH), 7.19–7.30 (m, 10 H, o-, m- and p-$2C_6H_5$), 8.17 (br, 3H, NH_3), 8.41 and 8.88 (each d, each 1H, H-3 and H-4, ^2J(H–H) = 8.0 Hz), 9.03 (s, 1H, H-6); ^{13}C (100.47 MHz, DMSO-d_8) δ (ppm): 41.9 (CH_2NH_3), 58.3 (CH_2OH), 123.6 (C-3), 127.1 (p-C_6H_5), 127.6 (m-C_6H_5), 131.8 (o-C_6H_5), 141.0 (C-5), 141.6 (C-2), 142.0 (C-6), 144.2 (C-4), 144.6 (br, i-C, C_6H_5), 163.2 (COOH), 163.9 (CO); ^{11}B (86.6 MHz, DMSO-d_6) δ (ppm): 10.8.

3. Results and discussion

3.1. NMR spectra

The treatment of 2-aminoethyl diphenylborinate whit methanol at −78 °C probably led to the formation of methyl diphenylborinate and ethanolamine, causing a transesterification reaction of a carboxylic acid group (2,3-pyridinedicarboxylic acid) with boron (methyl diphenylborinate) to take place [10], resulting in the formation of a boron compound. During formation of the boron compound and ethanolamine an acid–base reaction occurred between the other carboxylic acid group of the boron compound and ethanolamine. This acid–base reaction yielded diphenyl [(2-(3-carboxypyridyl))-carbonyloxy-O,N] boron (Scheme 1, **1**). The synthesis of diphenyl [(2-(5-carboxypyridyl))-carbonyloxy-O,N] boron (Scheme 2, **2**) was similar to that for **1** except that 2,5-pyridinedicarboxylic acid was used in the synthesis instead of 2,3-pyridinedicarboxylic acid.

Signals in the ^{13}C NMR spectrum of **1** were observed at 130.3 ppm for C_5, 135.6 ppm for C_3, 140.6 ppm for C_2, 140.9 ppm for C_6, 141.2 ppm for C_4, 145.3 ppm for the ipso-*C* atoms of both phenyl groups, and 162.5 ppm (C_2–*C*OO) and 166.8 ppm (C_5–*C*OOB) for the carboxyl carbon atoms. The carbon atoms on **1** were assigned with COSY and HETCOR spectra. The *C* atoms (C_2–*C*OOB) of **1** and **2** were determined due to increase in chemical shift values of *C*-atoms of *C*OOB group, when they are compared to that of 2,3- and 2,5-pyridinedicarboxylic acids. Signals corresponding to *C* atoms and protons of both phenyl groups were observed at the same shift values. Due to the use of DMSO as the solvent, the dative bond (B–N) could be eliminated by the solvent effect so that both phenyl groups were allowed to rotate freely, given that oxygen ligands have high affinities for boron [34,35]. In the ^{1}H NMR spectrum of **1**, multiple signals in the range of 7.20–7.29 ppm were observed from –B(C_6H_5)$_2$ group protons. A broad signal at 8.15 ppm was also observed for –C(NH^+_3) protons, a triplet signal at 7.98 ppm for the C_5-proton, a doublet at 8.23 ppm for the C_4-proton and a doublet at 8.87 ppm for the C_6–H proton. The B atom was observed at 10.2 ppm in the ^{11}B NMR spectrum of **1**. The chemical shifts in the ^{13}C NMR spectrum of **2** were different than those observed for **1**. Signals in the ^{13}C NMR spectrum of **2** were observed at 141.0 ppm for C_5, 135.6 ppm for C_3, 141.6 ppm for C_2, 142.0 ppm for C_6, 144.2 ppm for C_4, 144.6 ppm for the ipso-*C* atoms of both

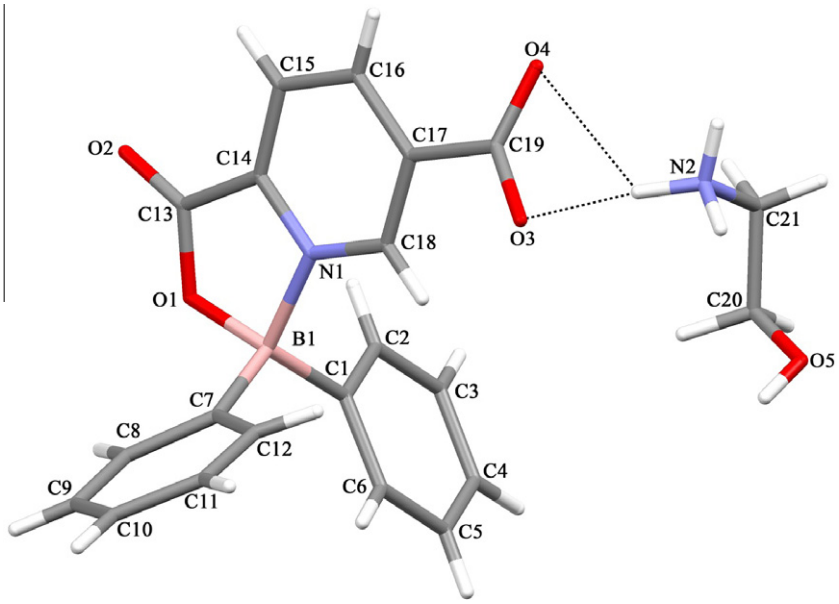

Fig. 5. The molecular structure of **2** with atom-labelling scheme.

phenyl groups, and 163.2 ppm (C_6-COO) and 163.9 ppm (C_5-COOB) for the carboxyl carbon atoms. Multiple signals in the ^{1}H NMR spectrum of compound **2** were observed in the range of 7.19–7.30 ppm for $-B(C_6H_5)_2$ group protons. There was also a broad signal at 8.17 ppm for $-C(NH^+_3)$ protons, a doublet signals at 8.40 ppm for the C_3-proton, a doublet at 8.88 ppm for the C_4-proton and a singlet at 9.03 ppm for the C_6-proton. A signal at 10.08 ppm was observed in the ^{11}B NMR spectrum of **2**.

3.2. FT-IR spectra

The broad bands at 3205 and 3287 cm^{-1} are attributed to ν(OH) of 2-ammoniumethanol for **1** and **2**, respectively. The absorption peaks at 3110 and 3175 cm^{-1} are assigned to $\nu(NH_3)$ stretching vibration of 2-ammoniumethanol ligand in **1** and **2**, respectively. The strong absorption bands at 1636, and 1648 cm^{-1} are due to ν(C=C) + ν(C=N) vibration of ligands for **1** and **2**, respectively. Several $\nu_{as}(COO^-)$ strong bands in free H_2pydc are shifted to lower frequencies of 1571 and 1431 cm^{-1} and 1568 and 1440 cm^{-1} in complexes **1** and **2**, respectively. The difference between the asymmetric and symmetric carboxylate stretching ($\Delta = \nu_{as}(COO^-) - \nu_s(COO^-)$) is often used for the correlation of the infrared spectra with the structures of metal carboxylates [36,37]. These values are approximately 228 cm^{-1} for monodentate, 164 cm^{-1} for ionic and 42 cm^{-1} for bidentate for carboxylate groups. These differences were determined for **1** Δ = 236 cm^{-1} (1571–1335 cm^{-1}, monodentate) and Δ = 162 cm^{-1} (1431–1269 cm^{-1}, ionic) and for **2** Δ = 239 cm^{-1} (1568–1329 cm^{-1}, monodentate) and Δ = 157 cm^{-1} (1440–1283 cm^{-1}, ionic). In the Na_2(pydc)·$n$$H_2O$ salt, these symmetric ν_s(COO) and asymmetric ν_{as}(COO) stretching bands were observed at 1402 and 1604 cm^{-1}, respectively. The absorption bands at 1335 and 1329 cm^{-1} correspond to B–O vibration of the compounds **1** and **2**, respectively [38].

3.3. Thermal analysis

The TG-DTG and DTA curves of **1** and **2** are shown in Figs. 1 and 2. The compounds **1** and **2** are thermally stable up to about 180 °C.

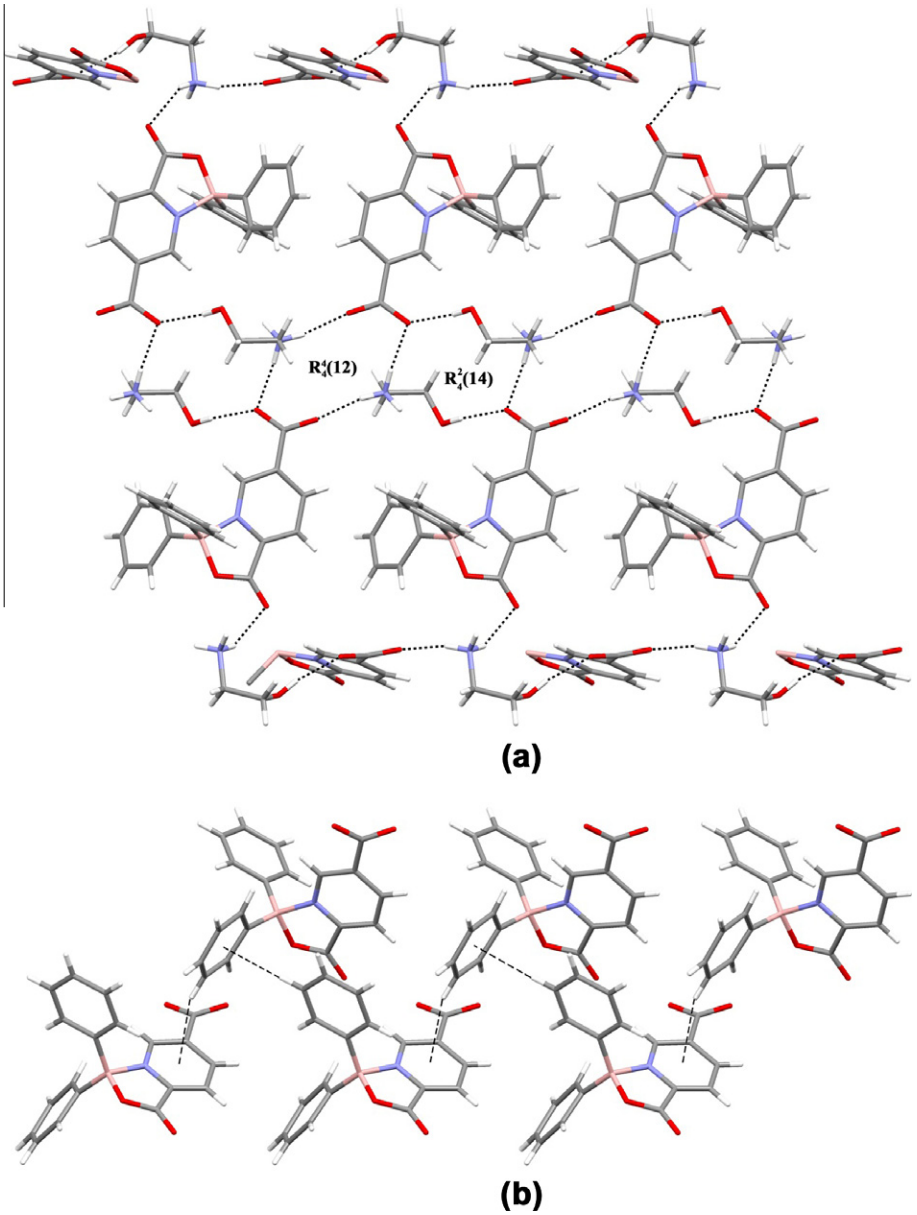

Fig. 6. (a) Inter-molecular hydrogen bonding of compound **2**. (b) Inter-molecular C–H···π interactions of compound **2**.

A two-step weight loss is observed upon further heating. The DTG curve shows two peaks at 216 and 261 °C for these stages. It is hard to give clear interpretations concerning degradation of organic groups because no flat plateau forms on TG curve. The rate of residue which is determined as 23.1% for **1** and 24.7% for **2** at 450 °C which is melting point for B_2O_3 shows that organic residues exist in the medium beside B_2O_3. As a matter of fact, only B_2O_3 would be expected to exist in the medium around 973 °C considering the literature [39–41] (Theoretic B_2O_3 17.8%). However, a constantly increasing mass loss occurs until 1300 °C starting from this temperature. This is an indicator that B_2O_3 and suboxides [41] formed of B_2O_3 start to evaporate above 450 °C. Thanks to FT-IR analysis of the remaining product of **1** (Fig. S1) we may state that 12% of the product at 1300 °C is a mixture of B_2O_3 and C [41].

3.4. Description of the crystal structures

The details of the crystal structures are given in Table 1. The molecular structure of **1** with the atom labelling is shown in Fig. 3. The selected bond lengths and angles and hydrogen bonding geometry are given in Tables 2 and 3. Compound **1** crystallizes in the monoclinic space group $P2_1/c$. The crystallographic analysis revealed that compound **1**, (Hea)[B(ph)$_2$(2,3-pydc)], consists of discrete [Ph$_2$B(2,3-pydc)]$^-$ anion and one protonated ea cation. The B atom has a distorted tetrahedral coordination and is chelated by the 2,3-pydc ligand through carboxylate O and pyridine N atoms. The tetrahedral geometry is completed by two *phenyl* groups. The B1–O1 (1.527(2) Å) and B1–N1 (1.595(2) Å) bond distances are similar to the corresponding values found in [B(ph)$_2$(pdca)] [10] (H$_2$pdca = 2,6-pyridinedicarboxylic acid), [BLSTc] [9] (L = 9-borabicyclo[3.3.1]nonane, STc = S-trityl-(R)-cysteine), [Ph$_2$C(NH$_2$)CO$_2$BPh$_2$].

The crystal packing of compound **1** is stabilized through strong intermolecular hydrogen bonding and C–H···π interactions, resulting in a 3D framework. The intermolecular N2–H22A···O3^{i}, N2–H22B···O2^{i}, O5–H10···O3^{ii}, N2–H22C···O4^{iii} and bonds have the H···O distances of 1.97, 2.18, 1.80 and 1.90 Å, respectively (Symmetry codes: (i) $-x+1, -y, -z+1$; (ii) $x, -y+½, z-½$; (iii) $-x+1, -y+1, -z+1$). It is seen from Fig. 4 that the hydrogen bonds between the Hea cations and the carboxylate groups of 2,3-pydc ligands, giving rise to $R_4^4(18)$ and $R_2^2(9)$ ring motives in the *bc* plane. These 2D layers are held together by C–H···π interactions to form a three-dimensional network. For the C8–H8···Cg contact (Cg = phenyl ring, C7–C12), the distance between atom H8 and the aromatic ring centroid is 2.81 Å, with a C18–H18···Cg angle of 141°. In **1**, the compound anion has A ring (N1/C14–C18), B ring (C1–C6) and C ring (C7–C12) plane and the dihedral angles between A–B rings, A–C rings and B/C rings are 58.79(7)°, 76.20(6)° and 68.06(7)°, respectively.

The structures of **2** (Fig. 5) is similar to that of **1**. The selected bond lengths and angles and hydrogen bonding geometry are given in Tables 2 and 3. As shown in Fig. 5, the boron ion in compound **2** is coordinated by a 2,5-pydc ligand and two phenyl groups, forming a significantly distorted tetrahedral geometry. The 2,5-pydc ligand acts as a bidentate chelating ligand, forming a five-membered ring [B–N1 = 1.624(4) and B–O1 = 1.524(3) Å]. The bond distances are comparable to those of compound **1**. The dihedral angle between the rings of pyridine and phenyl rings is 82.81(13), 69.54(13) and 80.92(13)°.

The individual molecules of **2** are connected by the N–H···O and O–H···O hydrogen bonds leading to two-dimensional hydrogen bonded layer (see Fig. 6a). The intermolecular N2–H2C···O2^{i}, N2–H2A···O4^{ii} and O5–H5···O3^{iii} bonds have the H···O distances of 2.10, 1.91 and 1.94 Å, respectively (Symmetry codes: (i) $-x+1, y-½, -z+½$; (ii) $-x+2, -y, -z+1$; (iii) $-x+1, -y, -z$). Some of these interactions are illustrated in Fig. 6b. These layers are held together by C–H···π interactions (C5–H5···Cg1 = 3.430(3) Å, 177; C9–H9···Cg2 = 3.820(3) Å, 155° and C21–H21A···Cg3 = 3.630(3) Å,

Table 4
The means of inhibition zone diameters of the two complexes against clinical and standard isolates of bacteria and clinical and standard isolates of yeast (disc Ø 6 mm).

	1			**2**			
	100 μg	150 μg	200 μg	100 μg	150 μg	200 μg	
Gram positive bacteria							
MRSA (clinical)	20	22	25	20	23	26	
B. subtilis	12	16	20	15	18	23	
B. cereus	13	15	20	15	18	22	
S. aureus	12	15	20	13	15	21	
Gram negative bacteria							
E. coli	–	7	8	–	7	8	
A. hydrophilia	14	16	20	15	18	21	
P. vulgaris	8	9	10	8	10	11	
E. fecalis	8	9	10	8	9	11	
VRE (clinical)	–	8	10	–	8	12	
	100 μg	150 μg	200 μg	100 μg	150 μg	200 μg	N
Standard yeast							
C. albicans	18	22	25	20	22	25	19
S. baulardii	7	9	10	8	10	13	20
R. rubra	18	20	23	19	20	24	21
Clinical yeast							
C. parapsilosis	18	21	25	18	21	25	20
C. tropicalis	10	12	15	12	16	18	15
C. krusei	16	20	24	8	12	15	10
C. globrata	8	10	14	9	13	16	20
C. albicans[a]	18	20	22	18	20	23	15
C. albicans[b]	15	20	26	15	22	28	20
C. albicans[c]	15	18	21	18	20	25	19

N, Nystatin (100 U/disc).

Table 5
Antimicrobial activity of standard antibiotics against microorganisms (disc Ø 6 mm).

Antibiotic discs	VA	E	C	IPM	RD	K	CTX	AMP	T	S	CN
Gram positive bacteria											
MRSA (clinic)	24	15	32	12	8	8	–	10	14	13	10
B. subtilis	22	30	29	30	26	21	30	26	35	20	17
B. cereus	17	22	25	30	18	19	10	9	27	22	18
S. aureus	20	25	20	39	25	20	8	29	25	20	20
Gram negative bacteria											
E. coli	12	15	30	40	20	20	40	25	24	20	15
A. hydrophilia	21	20	20	38	22	19	8	22	25	19	18
P. vulgaris	22	8	18	40	34	8	40	30	18	20	22
E. fecalis	18	19	24	30	24	11	28	28	12	20	14
VRE	–	16	12	20	12	–	–	21	34	18	–

Vancomycin (VA; 30 μg/disc), Erythromycin (E; 15 μg/disc), Chloramphenicol (C; 30 μg/disc), Imipenem (IPM; 10 μg/disc), Rifampicin (RD; 5 μg/disc, Kanamycin (K; 30 μg/disc), Cefotaxime (CTX; 30 μg/disc), Ampicillin (AMP; 10 μg/disc), Tetracycline (T; 15 μg/disc), Streptomycine (S; 25 μg/disc), Gentamisin (CN; 30 μg/disc).

127°, Cg1 = C7–C12, Cg2 = N1/C14–C18 and Cg3 = C1–C6) and hydrogen bonding interactions to form a three-dimensional network.

3.5. Antimicrobial activities

In the present study, *in vitro* potential antimicrobial activity of complexes **1** and **2** tested against microorganisms according to disc diffusion method is presented in Table 4. Antimicrobial activity was determined for 100, 150 and 200 μg/disc concentrations against tested microorganisms. The comparison of the obtained results with the 11 antibacterial agents and one antifungal agent used in the study are presented in Tables 4 and 5. Two complexes displayed antimicrobial activity against all tested microorganisms at 150 and 200 μg/disc concentrations. Two complexes did not display antimicrobial activity against *E. coli* and Vancomycin resistant *E. faecium* 100 μg/disc concentrations. Two complexes displayed maximum antimicrobial activity against MRSA at 200 μg/disc concentration. MRSA is a resistant variation of the common bacterium *S. aureus*. Inorganic and organic boron compounds possess interesting pharmacological properties, such as hypolipidemic, anti-inflammatory, anti-osteoporosis, and antineoplastic activities [8]. Two complexes displayed weak antimicrobial activity against *E. coli* (8 mm).

Complex **1** displayed antimicrobial activity against *B. subtilis*, *B. cereus*, *S. aureus*, *A. hydrophilia*, *P. vulgaris*, *E. fecalis* and Vancomycin resistant *E. faecium* (VRE) with diameters of zone inhibition ranging between 10 and 20 mm at 200 μg/disc concentration. Complex **2** showed antimicrobial activity against *B. subtilis*, *B. cereus*, *S. aureus*, *A. hydrophilia*, *P. vulgaris*, *E. fecalis* and Vancomycin resistant *E. faecium* (VRE) with diameters of zone inhibition ranging between 11 and 23 mm at 200 μg/disc concentration.

The MIC and MMC results of the two complexes against Gram positive and Gram negative bacteria are given in Table 6. Minimum Inhibitory Concentrations of the two complexes for the microorganism species ranged from 31.25 to 125 μg/mL. Two complexes exhibited activity against clinical MRSA with an MIC value of 31.25 μg/mL. Minimum microcidal concentrations of the two complexes for the microorganism species ranged from 250 to 500 μg/mL.

Two complexes displayed anticandidal activity against all standard and clinical yeasts at three concentrations (Table 4). Two complexes were found to be highly active against standard yeast *C. albicans* and less active against *R. rubra* and *S. baulardii*. Complex **1** was found to be highly active against clinical *C. albicans*[b] and less active against *C. parapsilosis* and *C. krusei*. It displayed low activity against *C. globrata* at 200 μg/disc concentration. Complex **2** was found to be highly active against clinical *C. albicans*[b] and less active against *C. parapsilosis* and *C. albicans*[c]. It displayed low activity against *C. krusei* at 200 μg/disc concentration. Obanda et al. [4] mentioned about fungicidal activity of boron in their study.

Minimal inhibitory concentration (MIC) and minimal microcidal concentration (MMC) results of the complexes against clinical and standard *Candida* species are presented in Table 6. MIC of complex **1** for the clinical and standard *Candida* species ranged from 62.5 to 125 μg/mL. MMC of the complex **1** for the microorganism species ranged from 125 to 500 μg/mL. MIC of the complex **2** for the clinical and standard *Candida* species ranged from 31.25 to 250 μg/mL. MMC of complex **2** for the microorganism species ranged from 250 to 500 μg/mL.

Table 6
Minimal inhibitory concentration (MIC) and minimal microcidal concentration (MMC) values of the complexes against clinical and standard isolates of bacteria and clinical and standard isolates of yeast.

	1		**2**	
	MIC (μg/mL)	MMC (μg/mL)	MIC (μg/mL)	MMC (μg/mL)
Gram positive bacteria				
MRSA (clinical)	31	250	31	250
B. subtilis	63	250	63	250
B. cereus	63	250	63	250
S. aureus	63	500	63	500
Gram negative bacteria				
E. coli	125	250	125	250
A. hydrophilia	63	250	63	250
P. vulgaris	125	250	125	250
E. fecalis	125	250	125	250
VRE (clinical)	125	250	125	250
Standard yeast				
C. albicans	63	250	31	250
S. baulardii	125	250	125	250
R. rubra	63	250	63	250
Clinical yeast				
C. parapsilosis	63	125	63	250
C. tropicalis	125	125	125	500
C. krusei	63	500	125	500
C. globrata	125	500	250	250
C. albicans[a]	63	250	63	250
C. albicans[b]	63	250	63	250
C. albicans[c]	63	250	63	250

Acknowledgments

This work was supported by Dumlupınar University, project No. 2007/14 and by Adnan Menderes University project No. FEF-08002.

Appendix A. Supplementary material

CCDC 770796 and 780575 contains the supplementary crystallographic data for **1** and **2**. These data can be obtained free of charge from The Cambridge Crystallographic Data Centre via www.ccdc.cam.ac.uk/data_request/cif. Supplementary data associated with this article can be found, in the online version, at doi:10.1016/j.ica.2011.11.006.

References

[1] V.D. Yumatov, E.A. Il'inchik, V.V. Volkov, Russ. Chem. Rev. 72 (2003) 1011.
[2] T.R. Chen, R.H. Chien, M.S. Jan, A. Yeh, J.D. Chen, J. Organomet. Chem. 691 (2006) 799.
[3] Y. Li, Y. Liu, W. Bu, J. Guo, Y. Wang, Chem. Commun. (2000) 1551.
[4] D.N. Obanda, T.F. Shupe, H.M. Barnes, Biores. Tech. 99 (2008) 7312.
[5] M.L. Ho, F.M. Hwang, P.N. Chen, Y.H. Hu, Y.M. Cheng, K.S. Chen, G.H. Lee, Y. Chi, P.T. Chou, Org. Biomol. Chem. 4 (2006) 98.
[6] J.J. Klappa, S.A. Geers, S.J. Schmidtke, L.A. MacManus-Spencer, K. McNeill, Dalton Trans. (2004) 883.
[7] N.J. Meltola, A.E. Soini, P.E. Hänninen, J. Fluores. 14 (2004) 129.
[8] S. Díaz, A. González, R.S. González, A. Rodríguez, J. Organomet. Chem. 610 (2000) 25.
[9] S.J. Baker, T. Akama, Y.-K. Zhang, V. Sauro, C. Pandit, R. Singh, M. Kully, J. Khan, J.J. Plattner, S.J. Benkovic, V. Lee, K.R. Maples, Bioorg. Med. Chem. Lett. 16 (2006) 5963.
[10] J. Trujillo, H. Höpfl, D. Castillo, R. Santillan, N. Farfán, J. Organomet. Chem 571 (1998) 21.
[11] P. Mahata, S. Natarajan, Eur. J. Inorg. Chem. 2005 (2005) 2156.
[12] M.R. Silva, P.S.P. Silva, A.M. Beja, J.A. Paixao, L.L.G. Justino, A.J.F.N. Sobral, J. Mol. Struct. 837 (2007) 58.
[13] X. Haitao, Z. Nengwu, X. Hanhui, W. Yonggang, Y. Rui, Y. Enyi, J. Xianglin, J. Mol. Struct. 597 (2001) 1.
[14] G.S. Fink, L.G. Cuervo, B. Therrien, H. Stoeckli-Evans, G.B. Shul'pin, Inorg. Chim. Acta 357 (2004) 475.
[15] P. Sengupta, S. Ghosh, T.C.W. Mak, Polyhedron 20 (2001) 975.
[16] G.H. Wang, Z.G. Li, H.Q. Jia, N.H. Hu, J.W. Xu, Cryst. Eng. Comm. 11 (2009) 292.
[17] H. Yin, S.X. Liu, J. Mol. Struct. 918 (2009) 165.
[18] Z.B. Han, Y. Ma, Z.G. Sun, W.S. You, Inorg. Chem. Commun. 9 (2006) 844.
[19] Z.B. Han, G.X. Zhang, J.W. Ji, P.J. Zhang, J. Chem. Crystallogr. 39 (2009) 169.
[20] Y. Kang, J. Zhang, Z.J. Li, J.K. Cheng, Y.G. Yao, Inorg. Chim. Acta 359 (2006) 2201.
[21] L.J. Lia, Y. Lia, J. Mol. Struct. 694 (2004) 199.
[22] M.A.S. Goher, A.A. Youssef, F.A. Mautner, Polyhedron 25 (2006) 1531.

[23] L.P. Sun, S.Y. Niu, J. Jin, G.D. Yang, L. Ye, Inorg. Chem. Commun. 9 (2006) 679.
[24] E.E. Sileo, O.E. Piro, G. Rigotti, M.A. Blesa, A.S. De Araujo, E.E. Castellano, Struct. Chem. 19 (2008) 651.
[25] A. Flores-Parra, R. Contreras, Coord. Chem. Rev. 196 (2000) 85.
[26] APEX2 and SAINT. Bruker AXS Inc., Madison, Wisconsin, USA Bruker (2007).
[27] G.M. Sheldrick, SHELXS-97; Acta Crystallogr. A46 (1990) 467.
[28] G.M. Sheldrick, SHELX-97, Universitat Gottingen, Germany, 1997.
[29] A.L. Spek, Platon-A Multipurpose Crystallographic Tool Utrecht, Utrecht University, The Netherlands, 2005.
[30] C.F. Macrae, P.R. Edgington, P. McCabe, E. Pidcock, G.P. Shields, R. Taylor, M. Towler, J. van de Streek, J. Appl. Cryst. 39 (2006) 453.
[31] National Committee for Clinical Laboratory Standards, Performance standards for antimicrobial disk susceptibility test, fourth ed., Approved Standard NCCLS Document M2-A4, vol. 10, No. 7, Villanova, PA, 1990; 9–15.
[32] National Committee for Clinical Laboratory Standard. Methods for dilution antimicrobial susceptibility tests for bacteria that grow aerobically, second ed., Approved Standard NCCLS Document M7-A2, vol. 10, No. 8, Villanova, PA, 1999; 12–15.
[33] National Committee for Clinical Laboratory Standards. Reference method for broth dilution antifungal susceptibility testing of filamentous fungi, Approved Standard (M38-A), NCCLS Document M38-A, vol. 22, No.16, Villanova, PA, 2002.
[34] G. Vargas-Díaz, H. Höpfl, J. Organomet. Chem. 694 (2009) 3660.
[35] H. Amt, W. Kliegel, S.J. Rettig, J. Trotter, Can. J. Chem. 68 (1990) 1797.
[36] L. Puntus, V. Zolin, V. Kudryashova, J. Alloys. Comp. 374 (2004) 330.
[37] K. Nakamoto, Infrared and Raman Spectra of Inorganic and Coordination Compounds, fifth ed., Wiley Interscience, New York, 1997.
[38] (a) R.W. Tilford, W.R. Gemmill, H.-C.Z. Loye, J.J. Lavigne, Chem. Mat. 18 (2006) 5296;
(b) A.P. Côté, A.I. Benin, N.W. Ockwig, M. O'Keeffe, A.J. Matzger, O.M. Yaghi, Science 18 (2005) 1166.
[39] D.A. Köse, B. Zümreoğlu-Karan, T. Hökelek, E. Şahin, Inorg. Chim. Acta 363 (2010) 4031.
[40] D.A. Köse, B. Zümreoğlu-Karan, O. Şahin, O. Büyükgüngör, J. Mol. Struct. 789 (2006) 147.
[41] H.E. Çamurlu, N. Sevinc, Y. Topkaya, J. Europ. Ceram. Soc. 28 (2008) 679.